NJC

Accepted Manuscript

This is an *Accepted Manuscript*, which has been through the Royal Society of Chemistry peer review process and has been accepted for publication.

Accepted Manuscripts are published online shortly after acceptance, before technical editing, formatting and proof reading. Using this free service, authors can make their results available to the community, in citable form, before we publish the edited article. We will replace this *Accepted Manuscript* with the edited and formatted *Advance Article* as soon as it is available.

You can find more information about *Accepted Manuscripts* in the Information for Authors.

Please note that technical editing may introduce minor changes to the text and/or graphics, which may alter content. The journal's standard Terms & Conditions and the Ethical guidelines still apply. In no event shall the Royal Society of Chemistry be held responsible for any errors or omissions in this *Accepted Manuscript* or any consequences arising from the use of any information it contains.

ROYAL SOCIETY OF CHEMISTRY

www.rsc.org/njc

NJC

RSC Publishing

ARTICLE

Novel sensor for sensitive determination of atropine based on Co_3O_4-reduced graphene oxide modified carbon paste electrode

Cite this: DOI: 10.1039/x0xx00000x

Received ooth January 2015,

DOI: 10.1039/x0xx00000x

www.rsc.org/

Hasan Bagheri,*[a] Seyedeh Maryam Arab,[b] Hosein Khoshsafar,[c] and Abbas Afkhami [d]

This paper has presented a novel strategy to carry out direct and sensitive determination of atropine in complex matrices based on the Co_3O_4-graphene modified carbon paste electrode. This novel nanostructure was characterized by different spectroscopic and electrochemical techniques including scanning electron microscopy, X-ray diffraction, Fourier transform infrared spectroscopy and electrochemical impedance spectroscopy. The fabricated electrochemical sensor showed good electrochemical response towards atropine. Under the optimized conditions, the calibration curve for atropine concentration was linear in the range from 0.1 to 3.2 μmol L^{-1} with the detection limit of 0.03 μmol L^{-1}. In addition, the practical analytical performance of the sensor was examined by evaluating the selective detection of atropine in biological fluids and pharmaceutical sample with satisfied recovery. Therefore, the prepared sensor may hold great promise for fast, simple and sensitive detection and biomedical analysis of atropine in various real samples.

Introduction

Quantitative analysis of pharmaceuticals is essential during various phases of drug development and during the fabrication stage, to ensure appropriate formulation, stability and quality. Other major fields include toxicology testing in pharmacology and in the clinical trial phase for monitoring bio-availability, pharmacokinetics and possible drug abuse.[1]

Atropine (AT) is health and life threatening alkaloid and thus the possibility of its quantitation is important in clinical and forensic toxicology. Such analyses represent quite a challenge for the analyst due to low concentrations in biological samples as well as because of the presence of high levels of interfering compounds. It has been commonly used in pharmaceutical preparations for the treatment of gastrointestinal diseases, cardiopathy and parkinsonism. [2] A high dosage of AT also stimulates the central nerve system. The most specific use of AT is an antidote to organophosphate cholinesterase inhibitors, found in certain insecticides and chemical warfare nerve agents like tabun (GA), sarin (GB) soman (GD). [3,4]

Despite these positive effects of AT against diseases, it is also a highly toxic compound. For instance, abnormal kidney function may lead to a toxic reaction in patients receiving AT treatment, therefore the dosage level of AT in pharmaceutical preparation is generally very low. For these reasons it demands sensitive and selective detection techniques. While the analysis of AT has historically been carried out by chemiluminescence, capillary electrophoresis, and liquid or gas chromatographic methods, [5,6] recent investigations have interested to electrochemical methods. [7-9] Mentioned above methods usually involve time-consuming and multi-step pretreatment including liquid–liquid extraction and/or solid-phase extraction to remove impurities contained in plasma or serum for the detection of this species. Also, these methods are expensive and not suitable for in-situ analysis due to the ponderous and complicated instruments. [10,11] Electrochemical methods enable several unique advantages including (1) ease of analysis due to a lack of the need for excessive sample preparation; (2) selectivity due to electrical signals at characteristic formal potentials, which can enable detection of multiple analytes without separation steps; and (3) the ability to analyse within biological matrices, including sweat, urine, serum, and cell culture media. Electrochemical methods also have reasonably fast sampling times, can offer valuable insights on the metabolic fate of the drug at particular dosage levels inside the body, and allow for investigations of the interaction of drugs with living cells.[1]

Limitations posed to electrochemical analysis include the need for significant electroactivity of the analyte of interest,

complications from interfering species that may be present at far higher concentration levels than the analyte of interest and signal drifts due to electrode fouling.

Electrochemical detection of AT concentrations at a bare electrode is not possible due to sluggish electron-transfer processes. To solve these problems, the use of chemically modified electrodes (CMEs) such as multiwall carbon nanotubes electrode, [7] screen printed graphite sensors, [9] and modified pencil graphite electrode, [8] instead of bare ones was suggested. The electrochemical performance of a CME is strongly affected by the electrode materials. [12-14] Chemically modified matrices should possess a high conductivity and a preferably low electron transfer resistance on their selective surface. Furthermore, it is also beneficial if there is a large surface area for interacting of target species. For these reasons, there is an emerging interest in nanostructured surfaces to be used in voltammetric determination. [12-17]

Graphene (Gr), a waved plane of sp^2-bonded monolayer carbon atoms perfectly arranged in a honeycomb lattice, has attracted fascinating interests across different disciplines. The considerable number of research reports emerged recently, underlining the importance of utilizing Gr for electrochemical sensors and proving the suitability of the material for the detection of some important species. [15-18]

However, the effective surface area of Gr materials depends highly on the layers, that is, single or few layers with agglomeration should be expected to exhibit a higher effective surface area. Therefore, numerous metal oxides and polymers have been added into Gr to enlarge the specific surface area of the pristine Gr. Also, nanoparticles have been shown to increase the electrode areas that could bring in more molecular recognition elements to improve the sensitivity of the sensor. Also, decorating Gr with nanoparticles leads to enhance in signal response. This is due to mutual interactions. [19,20] These composites are as effective strategies to improve the performance of electrochemical sensors. [21,22] Among the various metal oxide nanoparticles Co_3O_4 nanoparticles have recently gained more interest due to their low cost, biocompability, wide availability and excellent electrocatalytic properties. [19]

To the best of our knowledge, no study has reported the determination of AT using carbon paste electrodes (CPE). In the present work, we describe the findings of our continuing investigation of the properties of modified Gr composites.[15-17] The objectives of this work is to introduce an effective composite to design a sensitive and selective interface for electrochemical determination of AT in the presence of possible interferences by differential pulse voltammetry (DPV). So, we described the preparation and suitability of Co_3O_4-reduced Gr oxide /CPE as a new electrode for the determination of AT. The usefulness of the modified electrode with improved sensitivity and selectivity has been demonstrated for the applications in the pharmaceutical samples and biological fluids.

Experimental

Apparatus and chemicals

Fourier transform infrared (FT-IR) spectra were recorded in the range of 400-4000 cm^{-1} on a PerkinElmer, spectrum 100, FT-IR spectrometer. KBr pellet was used to prepare the samples for FT-IR measurements. The morphologies of composites were observed with a XL30 scanning electron microscope (SEM-EDX, Philips Netherland). X-ray powder diffraction (XRD, 38066 Riva, d/G.Via M. Misone, 11/D (TN) Italy) was employed to analyze the chemical components of the composites. Raman scattering was performed on a Almega Thermo Nicolet Dispersive Raman spectrometer. Electrochemical experiments were carried out at room temperature using a Behpajoh potentiostat/ galvanostat system (model BHP-2065). The electrochemical cell was assembled with a conventional three electrode system: a saturated calomel electrode (SCE) as a reference electrode (Azar electrode) and a platinum disk as an auxiliary electrode. Different working electrodes including CPE and modified CPEs were used. An Autolab electrochemical analyzer, Model PGSTAT 302 N potentiostat/galvanostat (Eco-Chemie, Netherlands), was used for impedance studies. The pH measurements were carried out using a Metrohm pH meter (model 713) with a combined pH glass electrode.

All chemicals and reagents used in this work were of analytical grade and used as received without further purification. Paraffin oil and graphite powder were obtained from Merck Company and used as received. AT Sulfate was prepared from Merck. Deionized distilled water (DDW) was used to prepare all the solutions. The commercial pharmaceuticals available from a local pharmacy were subjected to the analysis. Phosphate buffer, Britton-Robinson (B-R) universal buffer (0.04 M boric acid, 0.04 M acetic acid and 0.04 M phosphoric acid), acetate buffer and KNO_3 solution were prepared in DDW and were tested as the supporting electrolytes.

Synthesis of Co_3O_4/reduced Gr oxide nanocomposites

Gr oxide (GO) was synthesized by oxidation of graphite powder under acidic conditions according to the Hummer's method, [23] using a mixture of H_2SO_4, $NaNO_3$ and $KMnO_4$. In a typical synthesis of the Co_3O_4-reduced GO (rGO) hybrids, first, 0.93 g of cobalt acetate tetrahydrate ($Co(C_2H_3O_2)_2.4H_2O$) was dispersed in 20 mL of distilled water, and 0.3 g of GO was dispersed in 250 mL water by sonication for 2 h to achieve uniform dispersion of GO. Then, $Co(C_2H_3O_2)_2.4HO$ solution was gradually added to the GO solution. Meanwhile, 10 mL of ammonia solution (28%) were added to the above solution, which will be used for cobalt ion precipitation and GO reduction. Finally, the mixture was transferred into an autoclave for hydrothermal treatment at 180 °C under static condition for 12 h. The solid product was separated by centrifugation and washed thoroughly with water and absolute ethanol to remove any impurities. The product was labeled as Co_3O_4-rGO. For a comparison, pure Co_3O_4 and bare rGO were also synthesized in

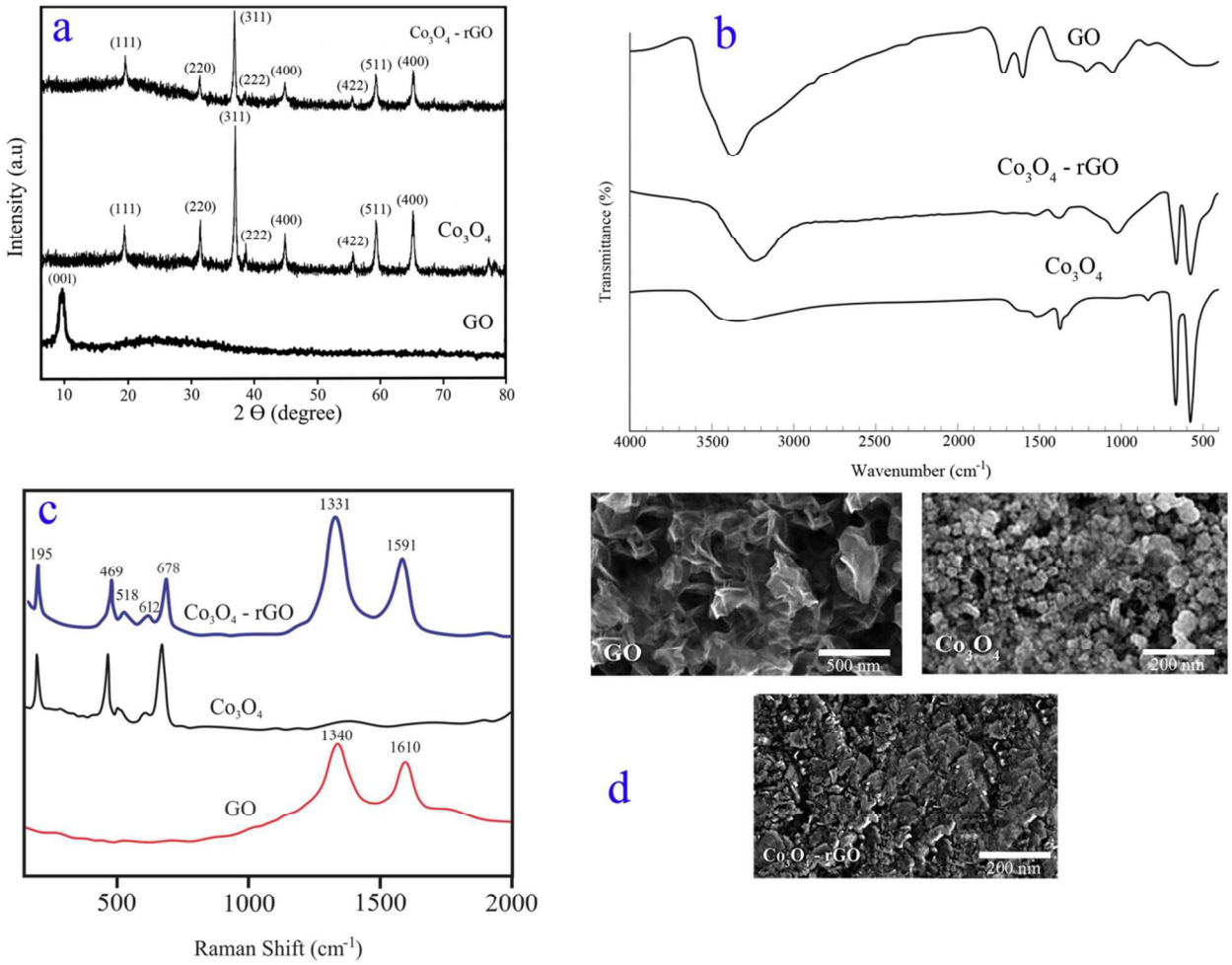

Fig. 1. Comparison of (a) XRD patterns, (b) FTIR spectra, (C) Raman spectra and (d) SEM images for GO, Co_3O_4 and Co_3O_4-rGO

the same way in the absence of Gr oxide or $Co(C_2H_3O_2)_2.4H_2O$. [24]

Preparation of the electrode

CPE electrode was prepared by thoroughly hand mixing of graphite powder with appropriate amount of paraffin oil in a mortar using a pestle (75:25,w/w%). A portion of the composite mixture was packed firmly a piston-driven carbon paste electrode holder. The Gr/CPE was prepared by mixing 10% (w/w) Gr, 65% (w/w) graphite powder and 25% (w/w) paraffin oil in a mortar and pestle. The mixture was homogenized and was used in the same way as the case of the unmodified electrode. The Co_3O_4-rGO/CPE was prepared by mixing the unmodified mixture with 14% w/w Co_3O_4-rGO and transferred into the CPE holder.

Preparation of real samples

This study was conducted by the Ethics Committee and written informed consents were obtained from a volunteer (he was from the co-authors). Human serum and urine samples were originally obtained from a non-smoking volunteer (male, 30 years, 80 kg and 175 cm). Also, the aliquot amounts of AT were added to biological samples which did not contain examined drugs. Urine samples were stored in a refrigerator immediately after their collection. 10 mL of the sample was centrifuged for 20 min at 2000 rpm. The supernatant was filtered using a 0.45 µm filter and then diluted 5-times with B-R buffer solution (pH= 10.0). The solution was transferred into the voltammetric cell to be analysed without any further pretreatment. Standard addition method was used for the determination of AT. The serum sample was centrifuged and then after filtering, dilute with B-R buffer solution (pH=10.0) without any further treatment.

Injection ampule samples were investigated under optimum conditions of experiment without any pretreatment.

Results and discussion

Surface characterization

The phase structure of synthesized samples was determined by XRD. The XRD patterns of GO, Co_3O_4 nanoparticles and Co_3O_4-rGO hybrids are shown in Fig 1a. The synthesized GO displayed a typical characteristic (002) peak at $2\theta=10^o$. The diffraction peaks of the Co_3O_4 are in good agreement with the standard Co_3O_4 (JCPDS card: 42-1467). [25] In the case of Co_3O_4-rGO the major diffraction peaks are well indexed with the cubic spinel Co, which are in good agreement with the standard card of Co_3O_4. The diffraction peak for C (002) in Gr oxide is invisible indicating that significant face-to-face stacking is broken due to the introduction of Co nanoparticles on both sides of Gr sheets. Additionally, no apparent additional peaks have been observed suggesting that the Co_3O_4-rGO composite is of high purity. [7] In addition, the broad peak at $2\theta=26^\circ$, corresponding to the stacked Gr sheets, was not observed, suggesting the decoration of Co_3O_4 nanoparticles could efficiently reduce the aggregation of the Gr sheets. As can be seen, the pattern of Co_3O_4-rGO displayed obvious diffraction peaks of Co_3O_4 nanoparticles, and the peak positions and relative intensities match well with the standard XRD data for Co_3O_4 nanoparticles, suggesting that prepared composite composed of pure crystalline Co_3O_4 nanoparticles were successfully decorated onto the reduced Gr sheets. The FT-IR spectra of the GO, Co_3O_4 nanoparticles and Co_3O_4-rGO composite (Fig. 1b) were also employed to confirm the chemical structure of prepared materials. The FT-IR spectrum of GO indicates that the broad absorption peak at 3360 cm^{-1} corresponds to OH group. The sharp peak at about 1600 cm^{-1} could be assigned to the C=C stretching of the aromatic ring. [26] The synthesized Co_3O_4 nanoparticles can be seen from the occurrence of strong absorption bands in the FT-IR spectrum, which encompass the characteristic wavenumbers at 500-600 and 600-700 cm^{-1} were assigned to Co-O vibrations. [27] FT-IR spectrum of Co_3O_4-rGO shows that the peaks at 625 and 560 cm^{-1} are denoted to stretching vibrations of Co–O–Co, clarifying the presence of cobalt oxide. Compared with GO, the intensity of absorption bands due to alkoxy, carboxy and carbonyl/ carboxy bonds disappeared or decrease. This clearly indicated that Co_3O_4 nanoparticles were successfully deposited on the surfaces of rGO.

In the Raman spectra of Co_3O_4-rGO and GO (Fig. 1c), the G band (~1600 cm^{-1}) corresponding to sp^2-hybridized carbon, and the D band (~1335 cm^{-1}) originating from disordered carbon is observed for both of the samples. The peaks of Raman shift at 195, 518, and 612 cm^{-1} can be attributed to the F_{2g} mode of Co_3O_4, and the peaks at 469 and 678 cm^{-1} can be attributed to the E_g and A_{1g} modes of Co_3O_4, respectively. These results demonstrate the existence of both Gr and Co_3O_4 in the as-prepared composites.[28]

SEM images of GO, Co_3O_4 nanoparticles and Co_3O_4-rGO are shown in Fig.1d. Significant differences in the surface structure of electrodes are observed. It can be seen that the structures of the GO is retained after introduction of metal nanoparticles. However, the surfaces of the Co_3O_4-rGO become much rougher than pure GO, indicating the growth of metal oxide nanoparticles on the surfaces. These particles are densely and homogeneously deposited with size range 20-40 nm.

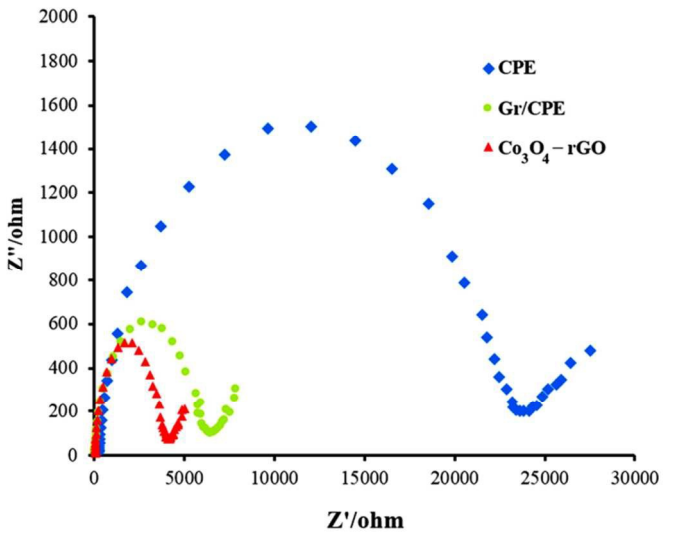

Fig. 2. Nyquist plots for various prepared electrodes in the 1.0 mmol L^{-1} $[Fe(CN)_6]^{4-/3-}$ and 0.1 mol L^{-1} KCl.

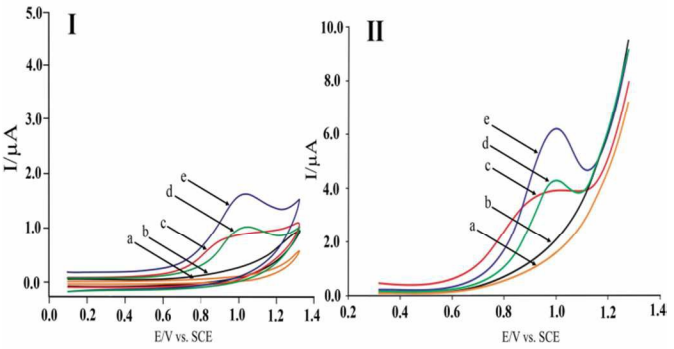

Fig. 3. (A) CVs (B) DPVs for 0.8 μmol L^{-1} AT in B-R buffer solution (pH=10.0) on the surface of various electrodes; curve (a) Co_3O_4-rGO/CPE in absence of analytes, (b) CPE, (c) Gr/CPE, (d) Co_3O_4/CPE and (d) Co_3O_4-rGO/CPE in presence of AT.

Electrochemical impedance spectroscopy (EIS) studies

As an available approach to monitor the interfacial properties the modified electrodes, EIS has been generally employed to characterize the modification steps. Fig. 2 shows the impedance spectra observed upon the stepwise modification process. The electron transfer resistance (R) of the electrode at different stages altered gradually with the successive modification, which were measured at a formal potential of 0.2 V versus SCE ($[Fe(CN)_6]^{3-/4-}$ et as the redox probe). CPE showed a high R value of 402 Ω. After the CPE was modified with Gr, the R was decreased to the value of 93 Ω, revealing the satisfactory electrical conductivity with the introduction of Gr. With the further modification by Co_3O_4-rGO, electrode surface showed a depressed semicircle with R value of 48 Ω, validating its high conductivity and fast electron conducting ability at the electrode surface.

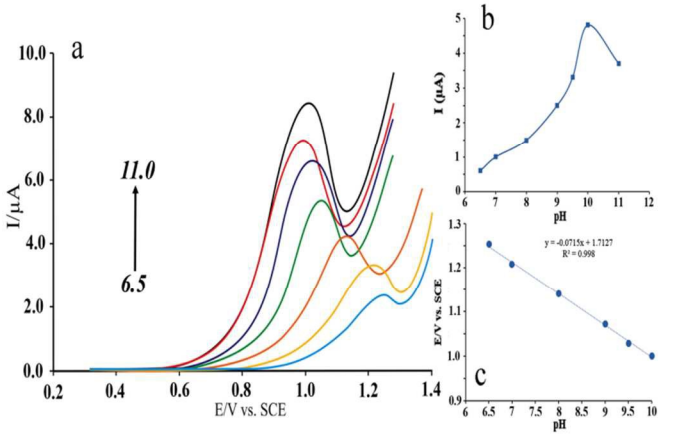

Fig. 4. (a) DPVs for Co_3O_4-rGO/CPE in 0.8 μmol L^{-1} AT at various pHs (pH 6.5, 7.0, 8.0, 9.0, 9.5, 10.0, 11.0). (b) Effect of pH on the peak currents. (c) Effect of pH on the peak potentials (pH 6.5-10.0).

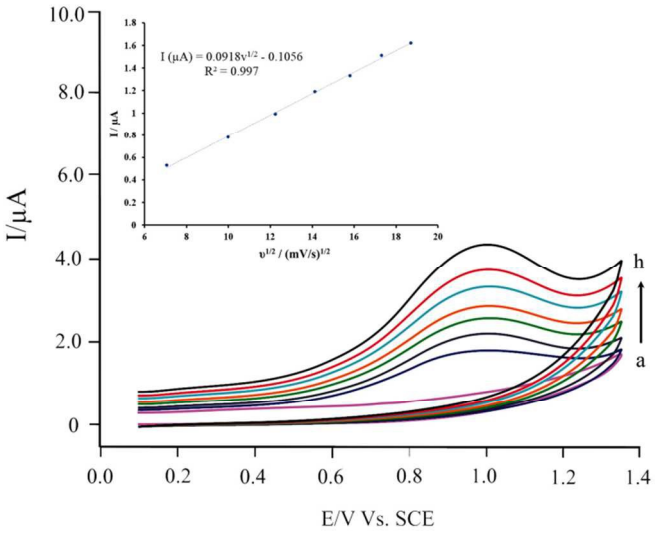

Fig. 5. CVs for Co_3O_4-rGO/CPE in B-R buffer of pH 10.0, a, and containing 0.5 μmol L^{-1} of AT with scan rates ranging from b to h as 50, 100, 150, 200, 250, 300, 350 mV s^{-1}, and Inset shows the linear relationship of the anodic peak current versus square root of the scan rate.

Electrochemical response of AT at the surface of various electrodes

To compare the performance of the prepared modified electrodes, the electrochemical response of AT was first studied on the surface of various electrodes using CV. Fig. 3I illustrates the cyclic voltammetric responses of 0.8 μmol L^{-1} AT in the B-R buffer (pH=10.0) with the scan rate of 100 mV s on the surface of the CPE, Gr/CPE, Co_3O_4/CPE and Co_3O_4-rGO/CPE, respectively. Cyclic voltammograms (CVs) at the CPE, did not exhibit any voltammetric peak (Fig. 3Ib). As it is shown in Fig. 3Ic, after the modification of electrode with Gr, an enhancement in the anodic peak current of AT was observed for the sensor (Gr/CPE: Ip = 0.25 μA). This increase in the current can be related to the increased active surface area of the electrode. An increase in response current occurs at the Co_3O_4/CPE in comparison with Gr/CPE due to strong enhancement in the electron transfer rate of AT (Fig. 3Id). Also, the apparent peak shape for AT at Co_3O_4/CPE is improved against at Gr/CPE, so that the well-shaped peak of AT can be observed with the presence of Co_3O_4 providing an excellent electrochemical reactivity. As can be seen in Fig. 3Ie, the anodic peak potential of AT is about 1.0 V vs. SCE. It was concluded, Co_3O_4-rGO/CPE is superior over other electrodes in terms of having a much higher response current for AT compared to other electrodes (Co_3O_4-rGO/CPE: Ip = 0.75 μA). An increase of 3 times was observed in the peak current of AT on the surface of Co_3O_4-rGO/CPE relative to Gr/CPE. Similarly, the CV of Co_3O_4-rGO/CPE is recorded in the absence of AT (Fig. 3Ia).

Fig. 3II shows the DPV responses of 0.8 μmol L^{-1} AT on the surface of the three above mentioned electrodes. As can be seen an obvious increase in the peak current and narrow peak was observed in the DPV response of Co_3O_4-rGO/CPE (curve 3IIe), indicating the increase in electron transfer rate. Moreover, the enhanced intensity of peak current can be due to the special structure and the large surface area of Co_3O_4-rGO/CPE. The above results indicate that Co_3O_4-rGO composite acts as a modifier incorporate with graphite and binder to fabricate a sensor with better electrochemical performance.

Effect of pH on the electrochemical oxidation of AT

In general, pH is one of the variables which commonly and strongly influences the current and shape of voltammograms. It is important to investigate the effects of pH on electrochemical systems. The differential pulse voltammetric response for 0.8 μmol L^{-1} AT was examined in B-R buffer (pH 6.5-11, Fig. 4a).

The peak current and potential were found to be markedly dependent on the pH. As can be seen from Fig. 4b with solution pH rising, the peak current increases, and it achieves a maximum at about pH 10.0, then decreases. The potential peak of AT is shifted with increasing pH between 6.5 and 10.0 (Fig. 4c) by a slope of 0.071 V/pH toward negative values. The linear regression equations are E(V) =1.71–0.071 pH, with the correlation coefficient 0.998. The slope of 0.071 V/pH for AT oxidation indicating that the number of electrons and protons involved in the reaction mechanism are not equal. A suggested pathway for possible oxidation of AT (1) consists of an initial electron transfer followed by proton loss to form the neutral radical (2), which could either lose an electron to form the imminium cation (3) is presented in Scheme 1. Then, the imminium cation would be expected to hydrolyze to give the product (4) which in turn decomposes to final product (5).[7,29,30]

Effect of scan rate

As we know, investigating the effect of scan rate on the oxidation peak current and peak potential can evaluate the kinetics of electrode reaction. CV experiments were carried out at different scan rates in order to investigate the electron-transfer process of the selected molecules on the Co_3O_4-rGO/CPE. All the CV experiments for AT was conducted in B-R buffer at pH = 10.0. The CVs recorded from 50–350 mV s^{-1}

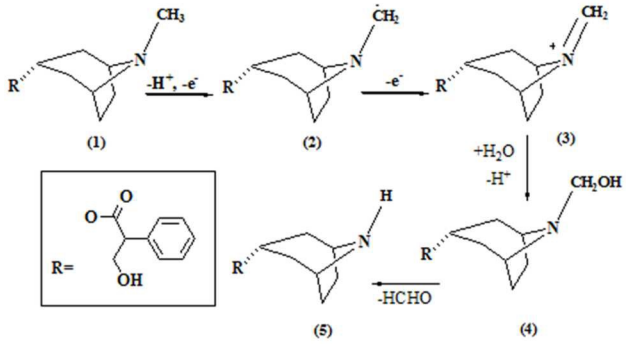

Scheme 1. Suggested oxidation mechanism for AT

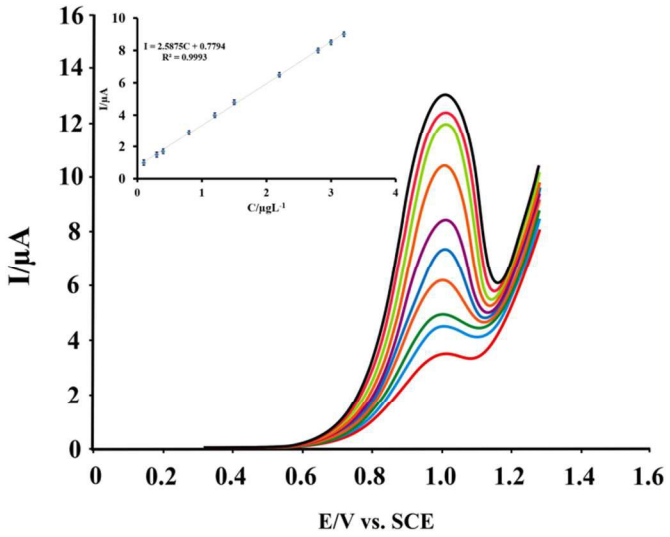

Fig. 6. DP voltammograms of different concentrations of AT in B-R (pH=10.0) and under optimum conditions. Inset shows the plot of peak current as a function of AT concentration in the ranges of 0.1-3.2 μmol L^{-1}.

Table 1 Results for AT determination (μmol L^{-1}) in various real samples obtained by the proposed method under the optimum condition.

Sample	Added	Found	Recovery (%)	Official Method
Urine	1.00	0.98	98.0	1.03
	2.50	2.44	97.6	2.48
Human serum	2.00	2.05	102.5	1.93
	3.00	2.96	98.6	3.02
Ampule	0.00	0.62	-	0.64
	0.50	1.11	98.3	1.12
	0.80	1.43	103.2	1.41

performed are shown in Fig. 5. The evaluation of the peak currents (I) as a function of the square root of the scan rate ($v^{1/2}$) revealed a linear relationship (see insets in Fig. 5), indicating

Table 2. Comparison of some characteristics of the proposed electrode with previously reported.

Electrode	Method	Linear range (μmol L^{-1})	Detection limit (μmol L^{-1})	Refs. No
Multi-wall carbon nanotube electrode	DPV	0.01-0.09	0.001	7
Modified pencil graphite electrode	DPV	0.6-30.0	0.03	8
Screen printed graphite sensors	CV	5.0–50.0	3.9	9
Co_3O_4–rGO/CPE	DPV	0.1-3.2	0.03	This work

that the electrode processes was governed by diffusion. Thus, rate-limiting adsorption and/or specific interactions at the Co_3O_4-rGO/CPE surface are negligible. The regression equations were as follows:

$I\ (\mu A) = 0.0918\ \upsilon^{1/2} - 0.1056\ (R^2=0.997)$ (For AT (oxidation))

Analytical performance

Under optimized condition, the applicability of the proposed voltammetric method to determine AT was examined by measuring the peak current as a function of concentration of the analyte. The linearity was checked by preparing standard solutions for 10 different concentrations of AT. The modified electrode demonstrated a linear response over range of 0.1-3.2 μmol L^{-1} with the coefficient R^2=0.999 (inset in Fig. 6). Although the linear range is narrow, it is common in electrochemical determination of AT. Even the previous papers in this field had not got wide linear range. [7-9]

Detection limit was estimated to be 0.03 μmol L^{-1} for AT based on $3s_b/m$, where s_b is the standard deviation of the mean value for 7 independent voltammetric response of the blank solution.

To determine the repeatability of the response of the modified electrode, electrochemical experiments were repeated 8 times with the same Co_3O_4-rGO/CPE in a 0.5 μmol L^{-1} AT solution. Relative standard deviation (RSD%) in the anodic peak current based on these replicates was calculated to be 3.1%. To evaluate the reproducibility of the electrode preparation procedure, 5 electrodes were prepared by the same fabrication process at different days and peak current of 0.5 μmol L^{-1} AT solution was measured by these electrodes. The RSD value for these peak currents was calculated to be 3.3%. After storing the electrode for 15 days under ambient conditions, the response of

fabricated sensor toward 0.5 μmol L^{-1} AT retained 94.8% of its initial response. These results indicate that the modified electrode has good repeatability, reproducibility and longtime stability in its voltammetric responses.

Interference studies

In order to evaluate the selectivity of the Co_3O_4-rGO/CPE sensor for the determination of AT, the influence of some common species on the determination of AT under the optimum conditions were investigated. The tolerance limit for interfering species was considered as the maximum concentration that gave a relative error less than 5.0% at a concentration of 0.5 μmol L^{-1} of AT. The interference effects of potentially interfering compounds, such as ascorbic acid (AA), uric acid (UA) and dopamine (DA) (which are present in biological fluids) were tested on the voltammetric response of AT (Fig. S1). No obvious change in the anodic peak current of AT was observed and the peaks of AA, DA and UA were well resolved from the anodic peak of AT, revealing the applicability of the modified electrode for electrochemical detection of AT in the presence of these compounds in real samples.

Also, the interference from the drugs which have clinical interaction with AT was investigated. Under optimal experimental conditions, additional 100-fold buffered salt (potassium chloride/sodium chloride), potassium citrate/sodium citrate, phentermine/topiramate, acetaminophen, chlorpheniramine, dextromethorphan, hyoscyamine and aspirine did not interfere with the voltammetric signal of AT.

In addition, glucose, lactose and sucrose showed no changes in the signals until up to 400 fold excess was used. This suggested that the determination of AT in the pharmaceutical and biological samples at Co_3O_4-rGO/CPE is not affected significantly by the common interfering species present along with the molecules of interest.

Real Sample Analysis

The applicability of the prepared modified electrode was tested by determination of AT in urine, serum and injection samples. The results presented in Table 1 indicated that the modified electrode retained its efficiency for the determination of AT in various samples with satisfactory results. Despite the presence of complex matrices in the studied real samples, they had no interference effects on the recovery percentage obtained by the suggested methods. Besides, the recovery studies of the spiked AT in samples showed average values in the range from 97.6 to 103.2% (Table 1), suggesting the successive applicability of the proposed strategy for the clinical applications. In addition, HPLC method was used for the analysis of the samples, to confirm the accuracy of the proposed method.

Conclusions

Electrochemical techniques have many advantages which make them an appealing choice for pharmaceutical analysis. To the best of our knowledge, no study has reported the determination of AT using CPEs. In the present study, a modified electrode was prepared using Gr nanosheet and Co_3O_4 nanoparticles on the surface of CPE. Electrochemical oxidation of AT was studied on the surface of these electrodes. Co_3O_4-rGO/CPE showed a better electrochemical response for AT compared with the Gr/CPE. This could be, due to high active surface area of the electrode. By applying Co_3O_4-rGO/CPE for voltammetric determination of AT, linear dynamic range of 0.1-3.2 μmol L^{-1} with the high sensitivity and selectivity and the low detection limit were obtained. Some figures of merit related to previous reports and the present study are shown in Table 2. The proposed method was used for determination of AT in biological fluids and pharmaceutical samples with acceptable recovery results, revealing the applicability of the method for real sample analysis. The prepared electrode with desirable electrochemical features such as good reproducibility and repeatability, good selectivity, acceptable long time stability of the electrode response and low cost together with the easy preparation of the modified electrode, could possibly be applied for pharmacokinetic studies, clinical analysis, quality control and routine determination of drugs in pharmaceutical formulations.

Acknowledgements

The authors gratefully acknowledge the support of this work by the Research Council Baqiyatallah University of Medical Sciences. They are grateful to Dr. Bardiya Jamali for his valuable suggestions.

Notes

[a] *Chemical Injuries Research Center, Baqiyatallah University of Medical Sciences, Tehran, Iran.*
[b] *Research Center of Shaygan Shimi Chemical Co.,Hamedan, Iran*
[c] *Young Researchers Club, Hamedan Branch, Islamic Azad University, Hamedan, Iran.*
[d] *Faculty of Chemistry, Bu-Ali Sina University, Hamedan, Iran.*

References

1. B. J. Sanghavi, O. S. Wolfbeis, T. Hirsch and N. S. Swami, *Microchimica Acta*, 2015, **182**, 1-41.
2. S. N. Azizi, M. J. Chaichi, P. Shakeri and A. Bekhradnia, *Journal of Luminescence*, 2013, **144**, 34-40.
3. T. C. Bania, J. Chu, D. Bailes and M. O'Neill, *Academic Emergency Medicine*, 2004, **11**, 335-338.
4. *Med Lett Drugs Ther*, 1990, **32**, 105-106.
5. B. Yuan, C. Zheng, H. Teng and T. You, *Journal of Chromatography A*, 2010, **1217**, 171-174.
6. S. Jakabová, L. Vincze, Á. Farkas, F. Kilár, B. Boros and A. Felinger, *Journal of Chromatography A*, 2012, **1232**, 295-301.
7. R. A. Dar, P. K. Brahman, S. Tiwari and K. S. Pitre, *Colloids and Surfaces B: Biointerfaces*, 2012, **91**, 10-17.
8. A. A. Ensafi, P. Nasr-Esfahani, E. Heydari-Bafrooei and B. Rezaei, *Talanta*, 2015, **131**, 149-155.
9. O. Ramdani, J. P. Metters, L. C. S. Figueiredo-Filho, O. Fatibello-Filho and C. E. Banks, *Analyst*, 2013, **138**, 1053-1059.

10. P. A. Steenkamp, N. M. Harding, F. R. van Heerden and B. E. van Wyk, *Forensic Science International*, 2004, **145**, 31-39.
11. A. C. Gören, G. Bilsel, M. Bilsel, S. Yenisoy-Karakaş and D. Karakaş, *Journal of Chromatography A*, 2004, **1057**, 237-239.
12. H. Bagheri, A. Afkhami, Y. Panahi, H. Khoshsafar and A. Shirzadmehr, *Materials Science and Engineering: C*, 2014, **37**, 264-270.
13. A. Afkhami, H. Bagheri, H. Khoshsafar, M. Saber-Tehrani, M. Tabatabaee and A. Shirzadmehr, *Analytica Chimica Acta*, 2012, **746**, 98-106.
14. H. Bagheri, A. Afkhami, H. Khoshsafar, M. Rezaei and A. Shirzadmehr, *Sensors and Actuators B: Chemical*, 2013, **186**, 451-460.
15. A. Afkhami, A. Shirzadmehr, T. Madrakian and H. Bagheri, *Talanta*, 2015, **131**, 548-555.
16. A. Afkhami, H. Khoshsafar, H. Bagheri and T. Madrakian, *Sensors and Actuators B: Chemical*, 2014, **203**, 909-918.
17. A. Afkhami, H. Khoshsafar, H. Bagheri and T. Madrakian, *Analytica Chimica Acta*, 2014, **831**, 50-59.
18. L.C.S. Figueiredo-Filho, D.A.C. Brownson, M. Gómez-Mingot, J. Iniesta, O. Fatibello-Filhoa and C.E. Banks, *Analyst*, 2013, **138**, 6354-6364.
19. C. Kaçar, B. Dalkiran, P. E. Erden and E. Kiliç, *Applied Surface Science*, 2014, **311**, 139-146.
20. L. Jiang, S. Gu, Y. Ding, D. Ye, Z. Zhang and F. Zhang, *Colloids and Surfaces B: Biointerfaces*, 2013, **107**, 146-151.
21. Z. Song, Y. Zhang, W. Liu, S. Zhang, G. Liu, H. Chen and J. Qiu, *Electrochimica Acta*, 2013, **112**, 120-126.
22. A. Gutés, C. Carraro and R. Maboudian, *Biosensors and Bioelectronics*, 2012, **33**, 56-59.
23. W. S. Hummers and R. E. Offeman, *Journal of the American Chemical Society*, 1958, **80**, 1339-1339.
24. Y. Yao, Z. Yang, H. Sun and S. Wang, *Industrial & Engineering Chemistry Research*, 2012, **51**, 14958-14965.
25. M. Wang, J. Huang, M. Wang, D. Zhang, W. Zhang, W. Li and J. Chen, *Electrochemistry Communications*, 2013, **34**, 299-303.
26. H.-L. Guo, X.-F. Wang, Q.-Y. Qian, F.-B. Wang and X.-H. Xia, *ACS Nano*, 2009, **3**, 2653-2659.
27. J. Jiang and L. Li, *Materials Letters*, 2007, **61**, 4894-4896.
28. B. Li, H. Cao, J. Shao, G. Li, M. Qu and G. Yin, *Inorganic Chemistry*, 2011, **50**, 1628-1632.
29. L.C. Portis, V.V. Bhat and C.K. Mann, *The Journal of Organic Chemistry*, 1970, **35**, 2175-2178.
30. B.L. Laube, M.R. Asirvatham and C.K. Mann, *The Journal of Organic Chemistry*, 1977, **42**, 670-674.

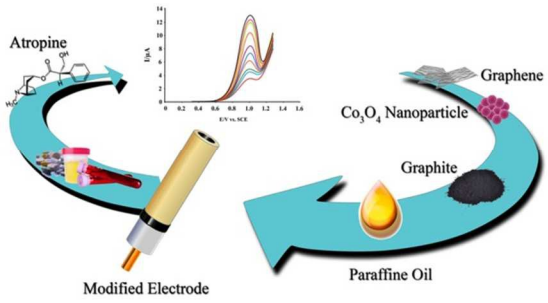

Co_3O_4-reduced graphene oxide acted as a selective and sensitive modifier in sensing layer for electrochemical determination of atropine.